



## Cleavage/fold relationships in the Silurian metapelites, southeastern Anglo-Brabant fold belt (Ronquières, Belgium)

T.N. Debacker<sup>1</sup>, M. Sintubin<sup>2</sup> & J. Verniers<sup>3</sup>

<sup>1</sup>Vakgroep Geologie en Bodemkunde, Universiteit Gent, Krijgslaan 281, S8, 9000 Gent, Belgium, e-mail: timothy.debacker@rug.ac.be

<sup>2</sup>Laboratorium voor Algemene Geologie, Katholieke Universiteit Leuven, Redingenstraat 16, 1000 Leuven, Belgium, e-mail: manuel.sintubin@geo.kuleuven.ac.be

<sup>3</sup>Laboratorium voor Paleontologie, Universiteit Gent, Krijgslaan 281, S8, 9000 Gent, Belgium, e-mail: jacques.verniers@rug.ac.be

Received 2 February 1999; accepted in revised form 27 February 1999

**Key words:** Acadian, progressive deformation, transecting cleavage

### Abstract

The presence of convergent cleavage fans in folded Silurian pelitic deposits along the southern extremity of the Brabant Massif has commonly been considered as an indication for a polyphase deformation history. Recent field work on the classic section at Ronquières shows, however, that all the structural elements can be explained by a single progressive deformation, taking place at gradually higher structural levels. This deformation is considered to have occurred at the time of the Acadian orogeny.

The section under study contains a fold train of five gentle to open first-order folds, unconformably overlain by gently S-dipping Givetian rocks. Although the Silurian turbidite deposits are predominantly pelitic, the folds are characterized by convergent cleavage fans. The trend of the cleavage fan axes remains constant in the various folds throughout the section. In contrast, the trend of the fold hinge lines gradually changes along the section from a clockwise relation with the cleavage fan axis in the northern part (anticlockwise cleavage transection) towards an anticlockwise relation in the southern part (clockwise cleavage transection). Individual fault/fault intersections have a constant trend throughout the section, parallel to the cleavage fan axes and the mean fold hinge line. Small kink bands and small transverse joints reflect the same structural trend.

The coaxial disposition of the structural elements seems at first sight incompatible with the presence of both clockwise and anticlockwise cleavage-transected folds. This disposition may, however, be explained by an echelon periclinal nature of the fold train, possibly formed in a slightly constrictional deformation environment.

### Introduction

The Lower Palaeozoic Brabant Massif (Belgium) forms the southeastern part of the predominantly concealed, NW–SE-trending, Anglo-Brabant fold belt (Lee et al. 1993). This belt is currently considered to have formed during the Early to early Middle Devonian (Van Grootel et al. 1997). Since its formation is synchronous with the Acadian orogeny in the Northern Appalachians, it is also described as such in the Irish, British and Belgian parts of the fold belt (cf. Soper et al. 1987, Woodcock 1991, Van Grootel et al. 1997).

The southern part of the Brabant Massif consists of an Ordovician–Silurian foreland basin, wrapped around a Cambrian core (Figure 1). In the fine-grained Silurian deposits of the southernmost part of this foreland basin a characteristic cleavage/fold relationship has been described (Mortelmans 1953, Vandeven 1967, Legrand 1967). In contrast to the more central parts, where the cleavage dip and the fold asymmetry both indicate a SW-verging tectonic transport (e.g., Lohest 1904, Fourmarier 1914, 1921), the southernmost area is characterized by open, upright folds with convergent cleavage fanning (*sensu* Ramsay

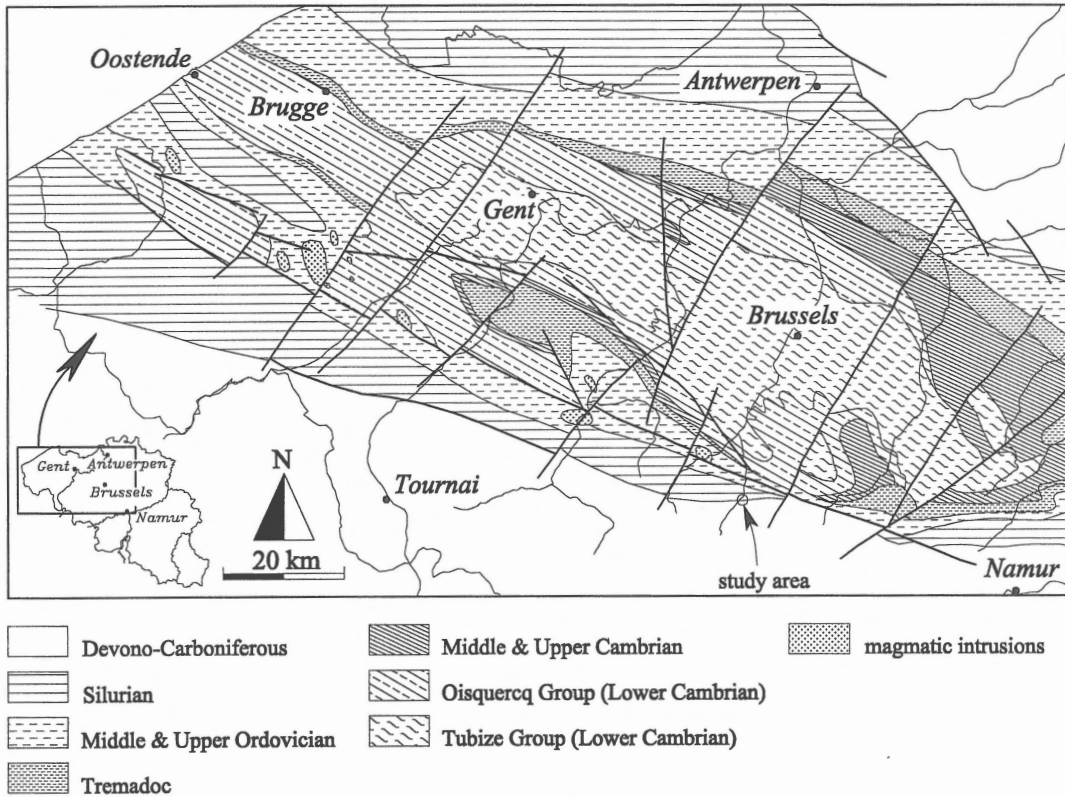


Figure 1. Geological subcrop map of the Brabant Massif (De Vos et al. 1993) showing the location of the study area.

1967). The convergent cleavage fans in these predominantly pelitic rocks have hitherto been explained by a polyphase deformation. A first-phase shortening, generating gentle buckle folds with a subparallel axial-planar cleavage, was supposedly followed by a minor second-phase shortening, causing the further amplification of the pre-existing folds, thus creating a fanning of the cleavage. While some authors, among them Mortelmans (1953) and Vandenven (1967), explained this particular cleavage/fold relationship as the result of a Variscan imprint on a folded Caledonian basement, Legrand (1967) invoked a polyphase Caledonian origin. The latter is based on observations in the Ronquières section, where the Devonian unconformity truncates the fold trains in the Silurian rocks, thus excluding a Variscan origin of the cleavage fanning.

In the Brabant Massif, this particular cleavage/fold relationship was observed only in the Orneau valley and along the Inclined Shiplift at Ronquières (cf. Legrand 1967). On both sides of the Inclined Shiplift, two 1.5-km-long sections, approximately at right angles to the overall structural trend, show folded Silurian deposits, unconformably overlain by gently

S-dipping Givetian deposits. The Silurian mudstones and siltstones, consisting of fine-grained distal turbidite sequences and hemipelagites of the Ronquières Formation (Gorstian, lower Ludlow, Louwey et al. 1992, Verniers et al. 1992), are anchizonal (Geerkens 1992) and show a penetrative cleavage. In contrast, the overlying Devonian rocks are nonmetamorphic and show no cleavage development.

By means of a detailed geometrical and fabric analysis of the section on the eastern slope of the Inclined Shiplift, this study aims to verify and refine the observations of Legrand (1967). Moreover, an attempt is made to assess the significance of the structural observations for the overall tectonic history of the southern margin of the Anglo-Brabant fold belt.

## Geometrical analysis

### *Fold geometry*

With the aid of bedding measurements and detailed logs of turbidite sequences (Verniers et al. 1992) a

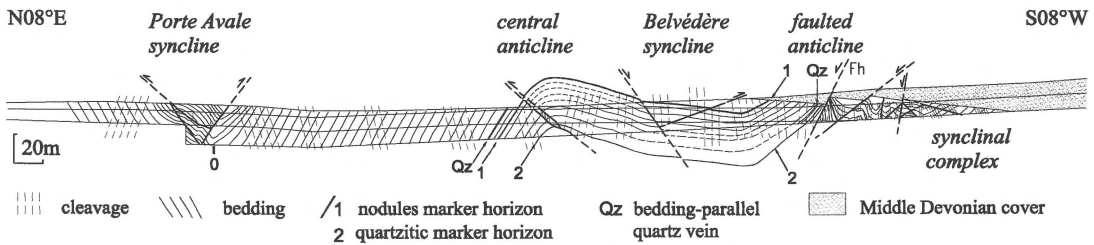


Figure 2. Cross-section of the Ronquières section on the eastern slope of the Inclined Shiplift. The lower entrance of the Inclined Shiplift is situated at point 0. To stress the thickness changes between the central anticline and the Belvédère syncline, the beds between the two marker horizons are extrapolated above and below the actual outcrop (hatched lines). Two footpaths running along the length of the outcrop (subhorizontal lines on section), separating three slope levels, are added for accurate location.

cross-section was constructed (Figure 2). It shows, from north to south, five gentle to open, upright to steeply inclined, subhorizontal to gently WNW-plunging first-order folds. In this order, these are the Porte Avale syncline, the central anticline, the Belvédère syncline (Verniers et al. 1992), a previously unnoticed faulted anticline and a strongly folded and faulted synclinal complex (cf. Legrand 1967). The three southernmost folds are truncated by the Devonian unconformity. The asymmetry of the folds is not uniform: the central anticline and the Belvédère syncline show a N-verging asymmetry, whereas the overall asymmetry of the synclinal complex is S-verging. On the northern limbs of the first-order synclines, small second-order (parasitic) folds are present. This is most pronounced in the synclinal complex and least in the Belvédère syncline.

In the gently S-dipping fold limb between the central anticline and the Belvédère syncline, a significant relative thickening is apparent (up to 35%). Logs of turbidite sequences show that, although present, sedimentological thickness variations alone cannot account for this thickening (Verniers et al. 1992, Verniers, unpublished data 1997). Fold-related thickness changes (thickened subhorizontal to gently dipping beds and strongly thinned steeply dipping beds) are also observed on meso- and microscopic scales in the synclinal complex.

The mean fold hinge line, determined on the basis of a best fit great circle through the poles of the bedding planes (pi-method), plunges gently towards the WNW (10/290). In detail, however, the plunge direction of the fold hinge lines gradually changes along the fold train from 295° in the north to 284° in the south (Table 1).

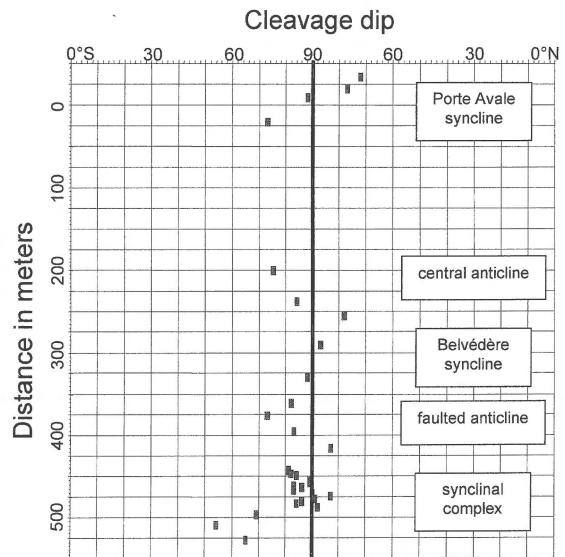


Figure 3. Diagram showing the change in cleavage dip (horizontal scale) with distance across the Ronquières section from N (-35 m) to S (550 m). The lower entrance of the Inclined Shiplift is situated at 0 m. The folds can readily be recognized from the change in cleavage dip.

### Cleavage geometry

In contrast to the predominantly N-dipping cleavage in the Brabant Massif (Legrand 1968), the cleavage in the Ronquières section dips on average to the south (Figure 3). The cleavage shows convergent fanning throughout the first-order folds, with a convergence angle of approximately 30° (cf. Legrand 1967). The cleavage fans approximately show a symmetrical disposition with regard to the axial planes. Cleavage fanning does not occur in the second-order folds.

Because of the fanning nature of the cleavage, stereographic projections allow the construction of virtual cleavage/cleavage intersections, which represent

*Table 1.* Orientation of cleavage fan axes (CFA) and fold hinge lines (FHL), the difference in trend (+ 00X°: CFA trending X° anticlockwise of the FHL, - 00X°: CFA trending X° clockwise of the FHL) and the difference in plunge between them. The measurements from the N-limb of the faulted anticline have been summarised with those of the Belvédère syncline and those in the southern limb with those of the synclinal complex. Due to a small angle between cleavage planes within some of the minor folds in the synclinal complex, no reliable CFA could be determined (/). In those cases (\*) the angle between the trend of the CFA and the FHL is assumed as being approximately equal to the difference in trend between the best fit girdle through the bedding poles and the average cleavage pole.

fold	fold hinge line (FHL)		cleavage fan axis (CFA)		trend difference CFA-FHL	plunge difference CFA-FHL		
Porte Avale syncline	13/295	(n = 107)	18/292	(n = 81)	+003°	05°		
central anticline	07/298	(n = 51)	09/114	(n = 40)	+004°	-16°		
Belvédère syncline	09/290	(n = 44)	05/292	(n = 51)	-002°	-4°		
Synclinal complex	anticline (441 m)	09/288	09/291	19/291	/	-003°	10°	/
	syncline (444 m)	(n = 335)	13/291	(n = 154)	/	-002°*	/	/
	anticline (447 m)		13/286	/	/	-005°*	/	/
	syncline (455 m)		04/288	32/294		-006°	28°	
	syncline (461 m)		11/286	29/290		-004°	18°	
	anticline (467 m)		10/289	23/291		-002°	13°	
	syncline (474 m)		11/285	14/291		-006°	03°	
	anticline (482 m)		07/282	12/291		-009°	05°	
	syncline (491 m)		13/284	14/291		-007°	01°	

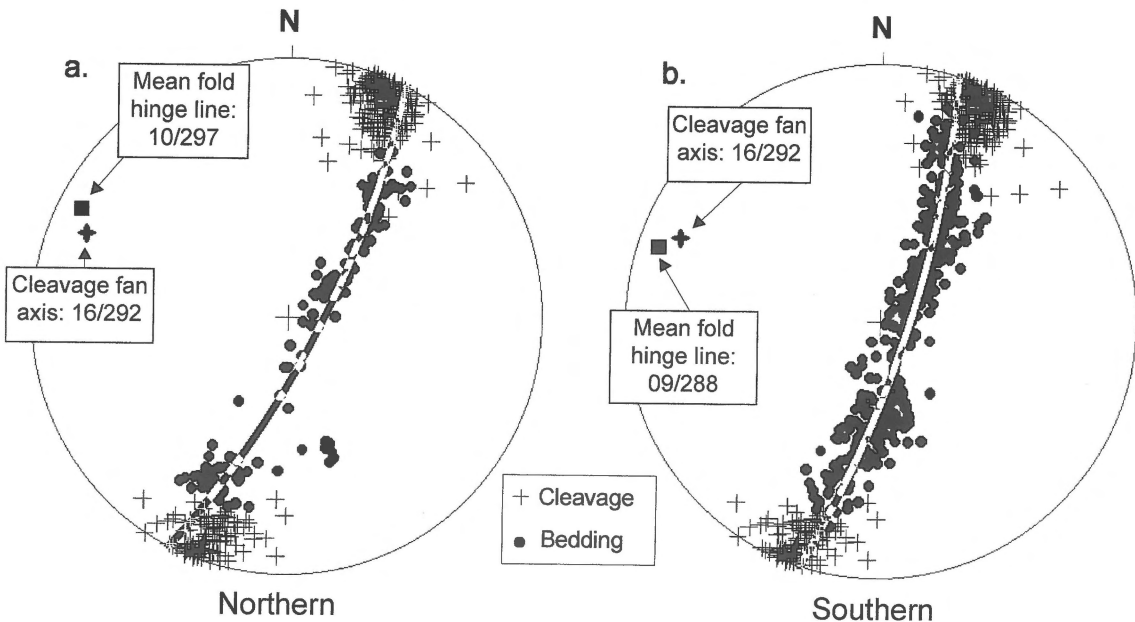


*Figure 4.* Lower-hemisphere equal-area projections showing the poles to bedding and to cleavage, the mean fold hinge line and the cleavage fan axis. (a) Data of the northern part of the section (Porte Avale syncline and central anticline). (b) Data of the southern part (Belvédère syncline, faulted anticline and synclinal complex). The poles to cleavage are identical in both plots.

the cleavage fan axes (CFA) (cf. Ramsay 1964). The term 'virtual' is used because cleavage/cleavage intersections are not present in outcrop. Note that, because of the small fanning angle, the plunge of the cleavage fan axes is poorly defined and therefore the trend of the cleavage fan axes will be used instead of its plunge direction. Contrary to the fold hinge lines, the trend of the cleavage fan axes remains constant throughout the outcrop (mean cleavage fan axis: 16/292) (Table 1). This results in an anticlockwise-transecting angular relationship of the cleavage fan axes with regard to the fold hinge lines in the northern part of the outcrop, and a clockwise relationship in the southern part of the outcrop (Figure 4). Only between the central anticline and the Belvédère syncline does the trend of the cleavage fan axis run parallel to the plunge direction of the fold hinge line (Table 1).

#### *Fault geometry*

The reverse faults in the Ronquières section all dip towards the north, according to Legrand (1967). Detailed logging of turbidite sequences by Verniers et al. (1992) revealed, however, the existence of both S- and N-dipping reverse faults. The present study revealed the presence of several more reverse faults. The faults often form conjugate sets and occur primarily in the fold cores. All shear sense indicators on fault planes indicate a pure dip-slip displacement. As indicated by the logs of turbidite sequences, the absolute reverse fault displacement never exceeds a few meters.

The normal faults seem to be confined to the southern part of the outcrop and cross-cut the Devonian unconformity, thus deforming the otherwise relatively undisturbed Givetian deposits. According to Legrand (1967), several of these faults are synsedimentary in origin. Apart from suggesting that at least some of these faults are reactivated inverted Caledonian faults, Legrand (1967) assumed an important lateral displacement on the normal fault which cuts the southernmost first-order anticline (Fh, Figure 2). No evidence for such a movement has been found, however, and striae on other fault planes all indicate pure dip-slip. In contrast to the other faults, Fh represents a significant break in the section. New logs of turbidite sequences from the synclinal complex cannot be correlated with those recorded on the other side of the fault (Verniers, unpublished data 1997). This indicates a minimum normal displacement of 25–30 m, which is more than the 5–10 m displacement indicated by the Devonian unconformity (cf. Legrand 1967). This implies that

normal-fault initiation predates the deposition of the Givetian. On the other hand, a minimum reverse displacement would have been in the order of 180 m (cf. Verniers et al. 1992). Considering the steep dip of Fh (66°) and the large minimum reverse displacement compared to the minimum normal displacement, a normal displacement seems energetically more feasible. It is therefore argued that the stratigraphic position of the beds in the synclinal complex is below that of the beds north of Fh.

The virtual fault/fault intersection plunges gently towards the WNW (10/290). In contrast to the fold hinge lines, no change in trend occurs across the section. Furthermore, the virtual intersection of the reverse faults is approximately parallel to the virtual intersection of the normal faults.

#### *Bedding-parallel slip planes*

A bedding-parallel, dm-thick quartz vein between a fine-grained sandstone bed (c-interval *sensu* Bouma 1962) and an underlying pelitic horizon (e-interval *sensu* Bouma 1962, cf. Verniers et al. 1992) in the steeply N-dipping limb of the central anticline can be ascribed to a bedding detachment due the competence contrast between these two different turbidite intervals. Thin bands of wall rock within the quartz vein indicate several episodes of slip and infill. Striae and slickensides indicate a pure dip-slip displacement and cleavage deflections in the adjacent beds point to a reverse movement. Whether this detachment is the result of thrusting or of flexural slip folding remains unknown. A similar quartz vein, with the same shear sense, is situated in the moderately to steeply N-dipping limb of the southernmost first-order anticline. Once again, this slip zone is situated between a thick fine-grained quartzitic sandstone and an underlying pelitic interval.

#### *Other structural elements*

Small, poorly developed, subhorizontal to gently inclined, compressional kink bands occur, locally causing a sigmoidal deformation of the cleavage. Most of these structures infer a top-to-the-south shear displacement, independent of their position in the overall structure. The mean strike of the axial surfaces of the kink bands is oriented WNW–ESE (286–106). This direction approximately matches the mean trend of the fold hinge lines, the cleavage fan axes and the fault/fault intersections.

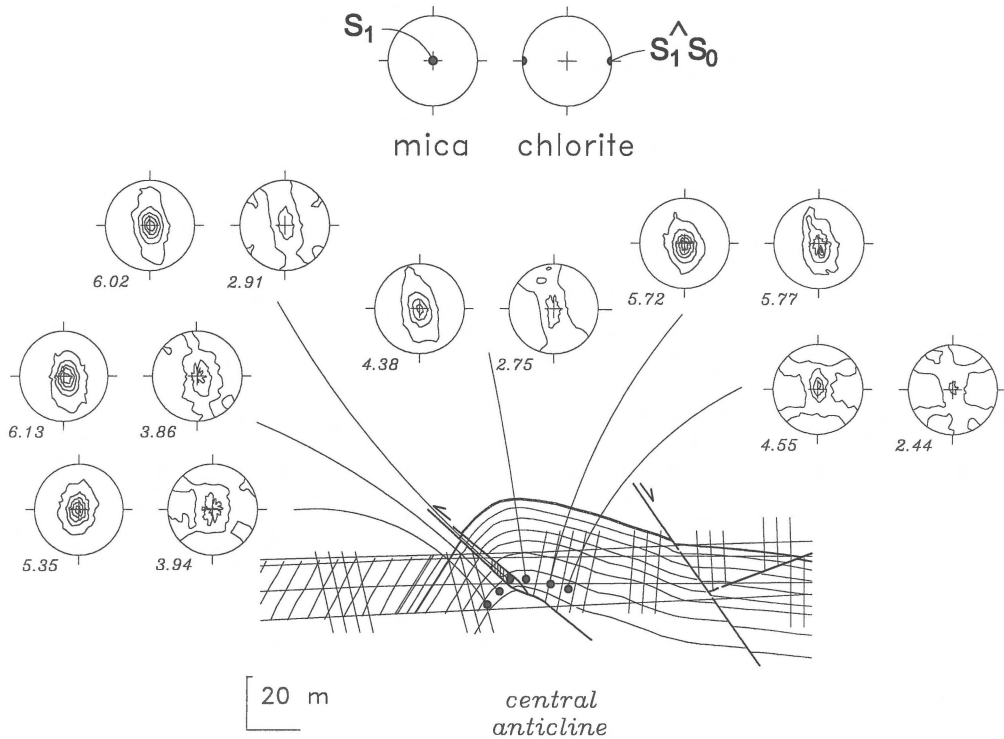


Figure 5. Central anticline: mica(001) and chlorite(002) pole-figure patterns (lower-hemisphere equal-area projections). All pole figures have been centred around the cleavage pole and have cleavage/bedding intersections in an E–W direction. For each sample, the mica(001) pole figures are presented on the left-hand side and the chlorite pole figures on the right. The degree of preferred orientation is expressed in multiples of a random distribution.

Apart from the large, roughly N–S-directed joints, small transverse NNE–SSW-trending joints are locally observed. The latter, so-called cross-joints (see Dennis 1967), are present in two sets with their line of intersection at right angles to the general structural trend. The W-dipping set dips more steeply than the E-dipping set.

## Fabric analysis

### *Cleavage fabric*

The predominantly pelitic material shows a homogeneous, fine-grained fabric, primarily composed of quartz, muscovite and chlorite. A spaced cleavage is apparent, locally showing crenulations of a bedding-parallel compaction fabric. Muscovite is concentrated in the cleavage domains, with a preferred orientation parallel to the cleavage. Chlorite, situated in the microlithons, is statistically oriented parallel to the bedding.

On six samples from a single bed across the central anticline, the phyllosilicate preferred orientation has been quantitatively evaluated using X-ray pole-figure goniometry (cf. Sintubin 1994). A consistent preferred orientation image emerges (Figure 5). There is no significant variation in the degree of preferred orientation nor is there in the pole-figure pattern across the anticline. A difference is observed, however, between the mica and chlorite orientation distributions. For both minerals, an intersection pole-figure pattern is apparent, reflecting the superposition of a cleavage fabric on a pre-existing, bedding-parallel, compaction fabric. The degree of preferred chlorite orientation is weak. The chlorite pole-figure pattern shows a clear girdle, with the cleavage/bedding intersection as symmetry axis. This pattern is characteristic of a crenulation fabric, in this case an incipient cleavage fabric on a bedding-parallel compaction fabric. Mica, on the other hand, shows a stronger degree of preferred orientation. The pole-figure pattern shows an orthorhombic symmetry, centred around the cleavage pole. The short axis of the orientation distribution still coincides

with the cleavage/bedding intersection, which means that there are still remnants of the bedding-parallel compaction fabric, even though mica is preferentially oriented parallel to the cleavage.

#### *Calcitic nodules*

In the turbidite and hemipelagic sequences of the northern part of the section, at least six bands of calcitic nodules are present. These nodules, restricted to a 3 m-wide stratigraphic level (Figure 2), are thought to be of diagenetic origin. In the subhorizontal to gently dipping beds in the Belvédère syncline, the nodules are prolate with their long axes approximately parallel to the fold hinge line. In the steep northern limb of the central anticline, however, the nodules are oblate with their short axes oriented roughly N–S. Similar oblate nodules, although occurring at a different stratigraphic level, are also present in the steep northern limb of the synclinal complex.

#### *Fracture infill*

The fractures, faults and bedding-parallel slip zones are infilled by secondary quartz, indicating that high fluid pressures prevailed during deformation (Price & Cosgrove 1990). Most of the quartz crystals are broken and truncated by small slip horizons. Dolomite is also present. It is well crystallized without truncations, indicating that it probably did not precipitate before the fault activity had ended. The joints also show traces of dolomite infill.

## **Discussion**

#### *Cleavage/fold relationships*

All structural elements in the Ronquières section point to a gently WNW-plunging structure ( $\sim 10^\circ$ ). The upright to steeply inclined, gentle to open, gently plunging folds show a gradual variation in plunge direction. The cleavage, on the other hand, has a rather regular attitude. The convergent cleavage fanning approximately shows a symmetrical disposition with regard to the fold hinges, clearly implying a genetic relationship. In the case of an axial planar convergent cleavage fan (i.e. no axial transection, *sensu* Johnson 1991), the cleavage fan axis is parallel to the fold hinge line. On the other hand, in the case of an axial cleavage transection, both the cleavage/bedding intersections and the cleavage fan axis are at an angle

with the fold hinge line. The angular discrepancy between the cleavage fan axes and the fold hinge lines in the Ronquières section clearly suggests an axial cleavage transection. Ideally, the sense of axial cleavage transection should be determined in subhorizontal, upright folds; the more the folds differ from this orientation (e.g. folds with steeply plunging fold hinge lines and gently inclined axial surfaces) the more care should be taken in determining the sense of transection (Johnson & Woodcock 1991). Considering the fold orientation in the Ronquières section (subhorizontal to gently plunging fold hinge lines and upright to steeply dipping axial surfaces), the trend difference between the cleavage fan axes and the fold hinge lines can readily be used as a measure of axial cleavage transection (Table 1). In the northern part of the outcrop, the cleavage transects the folds in an anticlockwise fashion, in the southern part of the outcrop in a clockwise fashion (Figure 4).

Following the ideas of Sorby (1853) concerning cleavage refraction, folds in competent materials have the tendency to show convergent cleavage fanning, whereas folds in less competent materials have the tendency to show divergent cleavage fanning (Ramsay 1967). The predominantly pelitic deposits in the Ronquières section can be considered as relatively incompetent. Therefore, the convergent cleavage fanning infers that – after completion of cleavage development – folding continued, passively rotating the cleavage and thus generating a convergent fan. This implies a single progressive deformation for the development of the convergent cleavage fans and contrasts with the two-phase models of Mortelmans (1953, Caledonian phase followed by a Variscan phase) and Legrand (1967, two separate Caledonian phases).

Numerous papers have equated cleavage-transected folds with transpressive deformation (e.g., Soper & Hutton 1984, Soper et al. 1987, Woodcock et al. 1988). Moreover, clockwise cleavage transection is often considered to indicate sinistral transpressive movements, whereas anticlockwise cleavage transection would indicate dextral transpressive movements. Does this imply a dextral transpressive component in the northern part of the Ronquières section and a sinistral component in the southern part? Considering the coaxiality of the other structural elements and the small scale of the outcrop, this possibility is rather unlikely. Furthermore, this association cleavage transection-transpression still remains a matter of controversy (e.g. Soper 1986) and, as Treagus & Treagus (1992) point out, the sense of cleavage transection

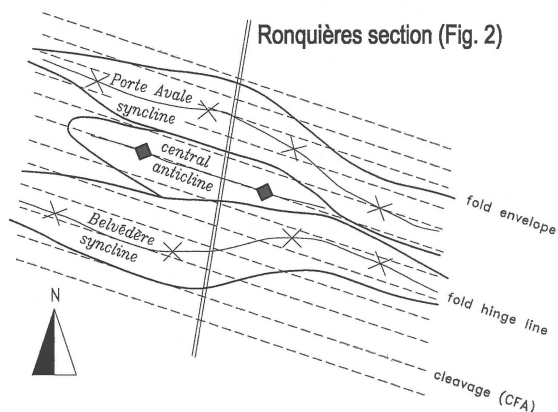


Figure 6. The fold train at Ronquières interpreted as an en-echelon periclinical fold assemblage (modified after Treagus & Treagus 1981) with nonaxial planar cleavage (not to scale).

in transpressive regimes depends, amongst other features, on the initial bedding orientation relative to the principal strain axes.

Another way to interpret this geometrical disposition of a regularly trending cleavage fan axis with regard to variably trending fold hinge lines is by applying a model of en-echelon periclinical folds with curving hinge lines, as put forward by Treagus & Treagus (1981) (Figure 6). Such en-echelon periclines imply that fold initiation took place on sedimentary layering oblique to the principal strain axes. On the other hand, fold hinge line migration most probably took place during a progressive deformation. Following the ideas of Treagus & Treagus (1981), such a geometrical disposition would infer a slight constrictional tectonic strain, which is seemingly in contradiction with the presence of a cleavage fabric, commonly considered as the reflection of a finite flattening strain. A slight constrictional tectonic strain on a bedding-parallel compaction fabric can, however, eventually generate a finite flattening strain.

This model is not the only way to explain the variable orientations of the fold hinge lines. If folds are large compared to initial bedding irregularities, at which they initiate, the fold hinge lines are expected to be approximately linear. If the folds are small relative to initial bedding irregularities, however, some variation in the fold hinge line orientations may be expected (Treagus, pers. comm. 1997).

#### Strain markers

The phyllosilicate pole-figure patterns basically reflect the polymodal nature of the crenulation fabric.

In such cases the March model (March 1932), which relates the phyllosilicate orientation distributions to strain, assuming passive rotation of platy fabric elements, cannot be applied (cf. Oertel 1983). In the case of the mica pole-figure patterns, however, a unimodal orientation distribution reflecting a cleavage fabric can be assumed (Figure 5). The degree of preferred mica orientation can therefore be used to give an estimate of the overall shortening associated with cleavage development. Based on the March model, the calculated shortening ranges between 39% and 45%.

The shape of the calcitic nodules clearly depends on their position in the fold structure. Oblate nodules are commonly present in the steeply N-dipping limbs, whereas the prolate nodules are only found in the gently S-dipping limb of the central anticline. This latter limb also experienced a significant relative thickening, predominantly of tectonic origin. Similar to the crenulation fabric, the prolate form of the nodules may result from a tectonic shortening associated with cleavage development, acting on initially slightly oblate nodules generated during compaction (cf. Giese et al. 1997). As such, the prolate nodules, the pole-figure patterns and the thickened limb are all indicative of a similar evolution. The oblate shape of the nodules in the steep limbs can be explained in a similar manner. Due to their steep dip, these limbs became relatively thinned, probably both during compaction and during shortening. As such, the initial slightly oblate shape of the nodules, formed during compaction, may have been preserved and accentuated by tectonic shortening.

#### *Relative chronology and shortening during the progressive deformation*

As argued above, the cleavage probably formed after fold initiation and a certain amount of buckling. Continued fold amplification passively rotated the cleavage, resulting in the formation of convergent cleavage fans. The kink bands, ductile to semi-ductile structures, deform the cleavage and are therefore post-cleavage. Their orientation and displacement sense are identical on both fold limbs, indicating that they formed after the main fold amplification. The faults cross-cut the folds and, unlike the kink bands, deform the cleavage in a brittle fashion. Thus, although fault initiation may have taken place as an accommodation structure during fold amplification, fault propagation is post-cleavage and appears to be post-fold amplification. Although no clear cross-cutting

relationships were observed between the reverse and normal faults we argue that normal faulting post-dates reverse faulting. Quartz precipitation took place during faulting, whereas dolomite precipitation probably occurred after faulting, since – in contrast to the quartz – the dolomite is unaffected by faulting. The cross-joints are believed to be the last structures formed. This seems to be confirmed by their dolomite infill.

The development of the structural elements can be seen as representing different increments of a single progressive deformation, a continuous deformation affecting the section at progressively higher structural levels, from folding and cleavage development in an early stage at lower levels to faulting and jointing in a later stage at higher crustal levels. Most of the deformation is definitely of Acadian origin and there are no clear indications for a Variscan or younger ductile tectonic imprint.

Although dealing with an unbalanced section (cf. Dahlstrom 1969, Hossack 1979), it can be attempted to restore the section, while assessing the significance of the different increments in the deformation history. In a first stage, the known fault displacements are removed. In a second stage, the folds are partly unfolded in order to obtain an assumed parallel cleavage throughout the outcrop. In the last stage, the remaining folds are completely unfolded. Due to geometrical problems (unknown fault displacements, the lack of continuous guide horizons), the synclinal complex could not be restored and hence the relative shortening only accounts for the part of the section north of the fault Fh. Consequently, the calculated shortening due to folding is probably too low. The total shortening is estimated at approx. 50%, mainly caused by cleavage development. The following relative chronology is proposed.

1. In a first stage, a fold train of gentle, upright folds was generated, with the local development of second-order parasitic folds. This initial shortening accounts for ~10%.
2. Based on the March model, the cleavage accounts for a shortening of ~40%.
3. After the completion of cleavage development, further fold amplification was responsible for the cleavage fanning and a supplementary shortening of ~6%. Small local kink bands probably developed during the last increments of this stage.
4. Conjugate fault sets are considered to accommodate the latest strain increments during fold amplification. These strain increments probably took

place at a higher structural level and account for only ~2% shortening.

5. Normal faulting and normal fault reactivation of pre-existing reverse faults, which also affects the Givetian cover, may be related to a post-orogenic collapse and Middle Devonian basin development south of the Brabant Massif. Probably the accompanying stress relaxation at this stage led to the development of the small NNE–SSW-trending cross-joints.
6. Finally, secondary dolomite, possibly derived from previously covering Frasnian deposits, precipitated in the remaining gaps within faults and fractures.

## Conclusions

Apart from the limited transecting nature of the cleavage, which can best be explained by an en-echelon periclinal disposition of the folds, a number of seemingly unrelated structural features show a striking coaxiality. This coaxiality is rather exceptional in the Ordovician–Silurian arc in the southern part of the Brabant Massif, where both to the east (clockwise cleavage transection) and to the west (anticlockwise cleavage transection) a transecting nature of the cleavage has been demonstrated (Sintubin 1997). The particular coaxial disposition in the Ronquières section suggests a frontal convergence in this part of the Brabant Massif. All the structural features in the section can be considered as the result of one single progressive deformation, taking place at gradually higher structural levels. This single progressive deformation is currently seen as the reflection of an Acadian deformation phase, acting on the Brabant Massif from the Early to early Middle Devonian (Van Grootel et al. 1997). The en-echelon periclinal folds with a non-axial planar cleavage may be indicative of slightly constrictional deformation conditions, acting on a bedding initially oriented oblique to the principal strain axes.

Currently, large-scale convergent cleavage fans in relatively incompetent rocks have only been described within the Silurian deposits along the southern extremity of the Brabant Massif, just north of the Silurian-Devonian unconformity (Mortelmans 1953, Legrand 1967). As demonstrated in the present contribution, a Variscan origin of the fanning (cf. Mortelmans 1953), which could explain the localised occurrence of the fans close to the Variscan deformation

front, can be ruled out. Instead, the particular spatial associations of the fans with open, upright fold trains might be related to the southward upthrusting of the Cambrian core of the Brabant Massif over its Ordovician–Silurian foreland basin.

The current work not only confirms and refines the observations of Legrand (1967), but also puts them into a new perspective by emphasizing the progressive and dynamic nature of the deformation, reflected in seemingly unrelated structural features.

## Acknowledgements

We are grateful to S.H. Treagus, N.H. Woodcock, H. Rondeel and F. Meilliez for critically reading the manuscript and giving constructive remarks. We would also like to thank G. Stoops for providing thin sections. The M.E.T.-D.231 Direction des voix hydrauliques de Charleroi is kindly acknowledged for the authorisation to study the outcrops along the Inclined Shiplift of Ronquières. T.N. Debacker is research assistant, M. Sintubin is postdoctoral fellow and J. Verniers is research director of the F.W.O.-Vlaanderen. This work forms part of the Research Project No. G.0084.97 of the F.W.O.-Vlaanderen.

## References

- Bouma, A.H. 1962 Sedimentary of some flysch deposits – Elsevier, Amsterdam
- Dahlstrom, C.D.A. 1969 Balanced cross sections – *Can. J. Earth Sci.* 6: 743–757
- Dennis, J.G. 1967 International tectonic dictionary, English terminology – A.A.P.G., Tulsa, Oklahoma
- De Vos, W., J. Verniers, A. Herbosch & M. Vanguetaine 1993 A new geological map of the Brabant Massif, Belgium – *Geol. Mag.* 130: 605–611
- Fourmarier, P. 1914 La poussée calédonienne dans le massif siluro-cambrien du Brabant – *Ann. Soc. Géol. Belg.* 41: 300–314
- Fourmarier, P. 1921 La tectonique du Brabant et des régions voisines – *Mém. Acad. Roy. Belg., Cl. Sc. (2e sér.)* 4: 1–95
- Geerkens, B. 1992 La cristallinité de l'illite dans le bord sud du Massif de Brabant – *Ann. Soc. Géol. Belg.* 115: 288–305
- Giese, U., G. Katzung, R. Walter & J. Weber 1997 The Caledonian deformation of the Brabant Massif and the Early Palaeozoic in northeast Germany: compared – *Geol. Mag.* 134: 637–652
- Hossack, J.R. 1979 The use of balanced cross sections in the calculation of orogenic contraction: a review – *J. Geol. Soc. London* 136: 705–711
- Johnson, T.E. 1991 Nomenclature and geometric classification of cleavage-transected folds – *J. Struct. Geol.* 13: 261–274
- Johnson, T.E. & N.H. Woodcock 1991 Detecting cleavage-transected folds using cleavage-bedding intersections – *J. Struct. Geol.* 13: 919–925
- Lee, M.K., T. Pharaoh, J. Williamson, C. Green & W. De Vos 1993 Evidence of the deep structure of the Anglo-Brabant Massif from gravity and magnetic data – *Geol. Mag.* 130: 575–582
- Legrand, R. 1967 Ronquières, documents géologiques – *Mém. Expl. Cartes Géol. Min. Belg.* 6: 1–60
- Legrand, R. 1968 Le Massif du Brabant – *Mém. Expl. Cartes Géol. Min. Belg.* 9: 1–148
- Lohest, M. 1904 Les grandes lignes de la géologie des terrains primaires belges – *Ann. Soc. Géol. Belg.* 31: 219–232
- Louwyse, S., G. Van Grootel & J. Verniers 1992 The stratigraphy of the type locality of the ?late Wenlock/early Ludlow Mont Godart Formation and the early Ludlow Ronquières Formation, Brabant Massif, Belgium – *Ann. Soc. Géol. Belg.* 115: 307–331
- March, A. 1932 Mathematische Theorie der Regelung nach der Korngestalt bei affiner Deformation – *Z. Kristall.* 81: 285–297
- Mortelmans, G. 1953 Efforts calédoniens et efforts hercyniens dans le Silurien de la vallée de l'Orneau – *Bull. Soc. Belg. Géol.* 62: 143–164
- Oertel, G. 1983 The relationship of strain and preferred orientation of phyllosilicate grains in rocks – *Tectonophysics* 100: 413–447
- Price, N.J. & J.W. Cosgrove 1990 Analysis of geological structures – Cambridge University Press, Cambridge
- Ramsay, J.G. 1964 The uses and limitations of beta-diagrams and pi-diagrams in the geometrical analysis of folds – *Quart. J. Geol. Soc. Lond.* 120: 435–454
- Ramsay, J.G. 1967 Folding and Fracturing of Rocks. McGraw-Hill, New York
- Sintubin, M. 1994 Textures in shales and slates. In: Bunge, H.J., S. Siegesmund, W. Skrotzki & K. Weber (eds) Textures of Geological Materials. DGM Informationsgesellschaft Verlag: 221–229
- Sintubin, M. 1997 Cleavage-fold relationships in the Lower Palaeozoic Brabant Massif (Belgium) – *Aardk. Meded.* 8: 161–164
- Soper, N.J. 1986 Geometry of anastomosing solution cleavage in transpression zones – *J. Struct. Geol.* 8: 937–940
- Soper, N.J. & D.H.W. Hutton 1984 Late Caledonian sinistral displacements in Britain: Implications for a three-plate collision model – *Tectonics* 3: 781–794
- Soper, N.J., B.C. Webb & N.H. Woodcock 1987 Late Caledonian (Acadian) transpression in north-west England: timing, geometry and geotectonic significance – *Proc. Yorks. Geol. Soc.* 46: 175–192
- Sorby, H.C. 1853 On the origin of slaty cleavage – *New Philos. J.* 55: 137–148
- Treagus, J.E. & S.H. Treagus 1981 Folds and the strain ellipsoid: a general model – *J. Struct. Geol.* 3: 1–17
- Treagus, S.H. & J.E. Treagus 1992 Transected folds and transpression: How are they associated? – *J. Struct. Geol.* 14: 361–367
- Vandenvén, G. 1967 Les remaniements de la schistosité des roches siluriennes dans la bordure méridionale du Massif du Brabant – *Ann. Soc. Géol. Belg.* 90: 519–531
- Van Grootel, G., J. Verniers, B. Geerkens, D. Laduron, M. Verhaeren, J. Hertogen & W. De Vos 1997 Timing of subsidence-related magmatism, foreland basin development, metamorphism and inversion in the Anglo-Brabant fold belt – *Geol. Mag.* 134: 607–616
- Verniers, J., S. Louwyse & G. Van Grootel 1992 Lithostratigraphical descriptions of the Mont Godart and the Ronquières Formations in their type localities and evaluation of the previous descriptions – *Prof. Pap. Geol. Surv. Belgium* 252: 1–67
- Woodcock, N.H., M.A. Awan, T.E. Johnson, A.H. Mackie & R.D.A. Smith 1988 Acadian tectonics in Wales during Avalonia/Laurentia convergence – *Tectonics* 7: 483–495
- Woodcock, N.H. 1991 The Welsh, Anglian and Belgian Caledonides compared – *Ann. Soc. Géol. Belg.* 114: 5–17